EBioMedicine 51 (2020) 102602

Contents lists available at ScienceDirect

EBioMedicine

journal homepage: www.elsevier.com/locate/ebiom

Research paper

# Tumour immune cell infiltration and survival after platinum-based chemotherapy in high-grade serous ovarian cancer subtypes: A gene expression-based computational study

Rong Liu[a,b,c,d,*], Rong Hu[e], Ying Zeng[a,b,c,d], Wei Zhang[a,b,c,d], Hong-Hao Zhou[a,b,c,d]

[a] Department of Clinical Pharmacology, Xiangya Hospital, Central South University, 87 Xiangya Road, Changsha 410008, PR China
[b] Institute of Clinical Pharmacology, Central South University, Hunan Key Laboratory of Pharmacogenetics, 110 Xiangya Road, Changsha 410078, PR China
[c] Engineering Research Center of Applied Technology of Pharmacogenomics, Ministry of Education, 110 Xiangya Road, Changsha 410078, PR China
[d] National Clinical Research Center for Geriatric Disorders, 87 Xiangya Road, Changsha 410008, Hunan, PR China
[e] Department of Obstetrics and Gynecology, Xiangya Hospital, Central South University, 87 Xiangya Road, Changsha 410008, PR China

ARTICLE INFO

*Article History:*
Received 8 September 2019
Revised 9 December 2019
Accepted 10 December 2019
Available online xxx

*Keywords:*
Tumour-immune infiltration
Platinum
High grade serous ovarian cancer
Overall survival
Progression-free survival

ABSTRACT

*Background:* Increasing evidence supports that the immune infiltration of tumours is associated with prognosis. Here, we sought to assess the relevance of the cellular composition of the immune infiltrate to survival after platinum-based chemotherapy amongst patients with high-grade serous ovarian cancer and evaluate these effects by molecular subtype.

*Methods:* We searched publicly available databases and identified 13 studies with more than 2000 patients. We estimated the proportions of 22 immune cell subsets by using a computational approach (CIBERSORT). Then, we investigated the associations between each immune cell subset and progression-free survival (PFS) and overall survival (OS), with cellular proportions modelled as quartiles.

*Findings:* A high fraction of M1 [hazard ratio (HR) = 0.92, 95% confidence interval (CI) = 0.86–0.99] and M0 (HR = 0.93, 95% CI = 0.87–0.99) macrophages emerged as the most closely associated with favourable OS. Neutrophils were associated with poor OS (HR = 1.06, 95% CI = 1.00–1.13) and PFS (HR = 1.10, 95% CI = 1.02–1.13). Amongst the immunoreactive tumours, the M0 macrophages and the CD8+ T cells were associated with improved OS, whereas the M2 macrophages conferred worse OS. Interestingly, PD-1 was associated with good OS (HR=0.89, 95% CI = 0.80–1.00) and PFS (HR=0.89, 95% CI = 0.79–1.01) in this subtype. Four subgroups of tumours with distinct survival patterns were identified using immune cell proportions with unsupervised clustering.

*Interpretation:* Further investigations of the quantitative cellular immune infiltrations in tumours may contribute to therapeutic advances.



## 1. Introduction

Ovarian cancer is the third leading cause of gynaecological cancer amongst women worldwide, with 295,414 new cases and 184,799 deaths predicted for 2018 [1]. Its advanced stage, the high-grade serous ovarian cancer (HGSOC) accounts for approximately 70% of the deaths [2,3]. The standard of care has not advanced beyond cytoreductive surgery and platinum-based combination chemotherapy. In addition, there has been little improvement in the overall survival (OS) of patients with HGSOC in the past three decades. Resistance to platinum treatment occurs in approximately 25% of patients with HGSOC within six months [4] after therapy, and the overall 5-year survival rate in the United States is 43.4% [5].

Great efforts have been made to explore the genomic changes in cancer cells and identify molecular abnormalities that influence the pathophysiology and constitute the therapeutic targets [6–9]. However, the functions of noncancer cells are still poorly understood because HGSOC tumours consist of complex mixtures of cancer and noncancer cells, including vascular cells, stromal cells and immune

*Abbreviations:* HGSOC, high grade serous ovarian cancer; OS, Overall survival; PFS, Progression-free survival; NK, natural killer; CIBERSORT, Cell type identification by estimating relative subset of known RNA transcripts; GEO, Gene Expression Omnibus; The Cancer Genome Atlas, TCGA; SVM, support vector machine; SD, standard deviation; HR, hazard ratio; CI, confidence interval; PAM, partitioning around medoid

* Corresponding author at: Department of Clinical Pharmacology, Xiangya Hospital, Central South University, Changsha 410008; P. R. China; Institute of Clinical Pharmacology, Central South University; Hunan Key Laboratory of Pharmacogenetics, Changsha 410078; PR China.
*E-mail address:* liuronghyw@csu.edu.cn (R. Liu).

https://doi.org/10.1016/j.ebiom.2019.102602

**Research in context**

*Evidence before this study*

Genomic features of tumors and tumour-associated cells represent promising biomarkers of clinical outcome. Deeper understand of the tumour immune microenvironment, which be comprised with an intricate system of immune cells, is likely to reveal advanced prognostic biomarkers and novel targets for therapeutic modulation. Rapidly emerging evidence suggests that a favourable tumour immune cell infiltration underpins mounting robust antitumor responses and better clinical results after treatments. Previous studies have shown that ovarian tumour-infiltrating lymphocytes are associated with prognosis. However, whether particular immune cell types are associated with a greater or lesser risk of disease progression or death and how these effects differ by ovarian cancer subtype, remains unclear. Our study made full use of public data for HGSOC patients treated with platinum-based chemotherapy. We systematically searched Gene Expression Omnibus (GEO https://www.ncbi.nlm.nih.gov/geo/), The Cancer Genome Atlas (TCGA, https://portal.gdc.cancer.gov/) and ArrayExpress (https://www.ebi.ac.uk/arrayexpress/) with the keywords 'ovarian cancer' and 'survival'. In total, 28 studies were identified. Finally, 2218 patients from 13 studies (Table S1) were included in subsequent data analysis after filtering patients with stage I or grade I ovarian cancer, or without serous ovarian cancer, or not treated with platinum-based chemotherapy, or without available survival information.

*Added value of this study*

We found high fraction of M1 and M0 macrophages cells emerged as the most closely associated with favourable OS. Neutrophils were associated with poor OS and PFS. amongst immunoreactive tumours, M0 macrophages and CD8+ T cells were associated with improved OS, while M2 macrophages were associated with worse OS. High expression of PD-1 was associated with better OS and PFS in the immunoreactive subtype, suggesting patients within this subtype might benefit from cancer immunotherapies. Neutrophils were associated with poor PFS within mesenchymal subtype. In proliferative subtype, T cell gamma delta, resting mast cells and activated CD4 memory T cells were associated with poor PFS, while activated mast cells were associated with favourable PFS. Four subgroups of tumours with distinct survival patterns were identified using immune cell proportions with unsupervised clustering.

*Implications of all the available evidence*

Our study highlights the positive association between tumour immune infiltration with M0 and M1 macrophages and better prognosis on a genomic level. We observed that neutrophils were associated with poor prognosis. In the immunoreactive subtype, CD8+ T cells and higher expression of PD1 were associated with improved OS. We found differences exist in the cellular composition and molecular subtypes of the immune infiltrate in HGSOC tumours, and could possibly be critical determinants of survival after platinum chemotherapy. Further quantitative investigations of cellular immune infiltrations in tumours may make contributions to therapeutic advances.

cells. Immune cells seem to have potential to be targeted by drugs for improved prognosis. Pieces of evidence have demonstrated the importance of tumour infiltration in immune cells, such as tumour-associated macrophages and dendritic, helper T and cytotoxic T cells, in tumour progression, therapeutic responses and prognosis [10,11]. The changes in the numbers of macrophages and CD8+ T cells infiltrating the tumour microenvironment are associated with prognosis and treatment response in various malignancies, including melanoma, hepatocellular carcinoma and breast and lung cancers [12–15]. Cancer immunotherapies by immune checkpoint blockades (such as PD-1, PDL-1 and CTLA-4) can help recognise and attack the cancer cells of the immune system [16,17]. The use of immune checkpoint blockades can significantly prolong the survival time of a portion of patients with solid tumours, such as melanoma [18]. An increasing body of literature have proven that the presence of tumour-infiltrating lymphocytes confers favourable prognosis in patients with ovarian cancer [19–21]. However, these studies are limited to only one or two immune cell types because histologically quantifying the individual tumour infiltrate immune cell subsets in a large cohort is a difficult and laborious due to the variety of specialised immune cell types. In addition, investigations on the prognostic value of tumour-infiltrating immune cells in HGSOC following platinum-based chemotherapy in a systematic manner are lacking. Enumerating immune cells that can represent the breadth of their specialised characteristics to some extent is essential to deeply understand the nature and diversity of immune responses to platinum-based treatment of HGSOCs. Moreover, conducting a pooled analysis with large-scale public cohorts of samples covering the molecular diversity of HGSOC is necessary to reliably test the association between the immune cell subsets and the prognosis within the molecular subtypes of HGSOC.

This study aims to quantify the cellular composition of the immune response in HGSOC to explore its association with OS and PFS after platinum-based chemotherapy in general and by HGSOC molecular subtype. The gene expression deconvolution algorithm [cell type identification by estimating the relative subset of known RNA transcripts (CIBERSORT)] [22] was utilised to estimate the relative fractions of 22 distinct functional immune cell subsets based on mixed cellular gene expression data in 2218 unrelated HGSOC transcriptomes with known clinical follow- from public datasets.

## 2. Materials and methods

### 2.1. Study population and eligibility criteria

Our study made full use of publicly available datasets. The Gene Expression Omnibus (GEO, https://www.ncbi.nlm.nih.gov/geo/), The Cancer Genome Atlas (TCGA, https://portal.gdc.cancer.gov/) and ArrayExpress (https://www.ebi.ac.uk/arrayexpress/) were systematically searched using the keywords 'ovarian cancer' and 'survival' to identify the gene expression dataset of patients with HGSOC, who underwent platinum-based chemotherapy. In total, 28 studies were identified. Finally, 2218 patients from 13 studies (Table S1) were included in subsequent data analysis after filtering patients with stage I or grade I serous ovarian cancer, untreated with platinum-based chemotherapy, or with survival information unavailable. The exclusion criteria can be found in Table S2. The statements regarding patient consent and ethical approval for all studies used here are listed in their original corresponding articles. The detailed information of which samples were utilised at each phase of statistical analysis is shown in Fig. 1.

The normalised expression data in a series matrix format (as uploaded by the authors) and relevant clinicopathological data, treatment regimen and survival were retrieved from GEO. For datasets without clinical information in combination with the gene expression profiles, the supplementary information of the original publication was searched. For each sample, probe sets without a specific gene annotation were filtered. When multiple probe sets correspond to a

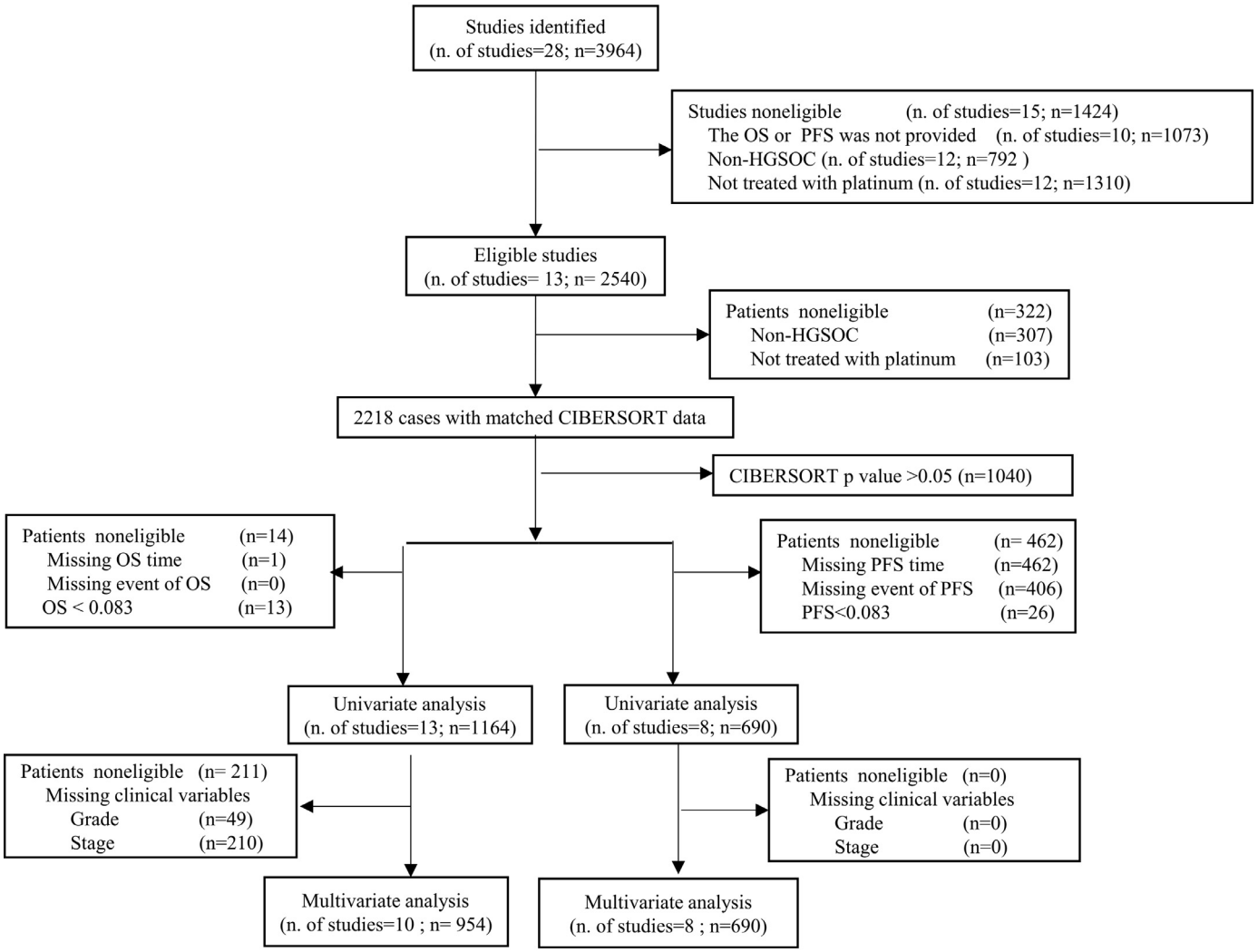


**Fig. 1. Study flowchart detailing which samples were utilised at each stage of statistical analysis.** HGSOC, high grade serous ovarian cancer; OS, overall survival; PFS, progression-free survival.

single gene, the average value of all probe sets mapped to the gene was used.

### 2.2. Molecular subtyping

The report from TCGA research network revealed four HGSOC molecular subtypes identified by a consensus non-negative matrix factorisation analysis of gene expression levels, namely, 'Differentiated', 'Mesenchymal', 'Immunoreactive' and 'Proliferative' [6]. Furthermore, Verhaak et al. developed subtype gene expression signatures with 100 marker genes from 1500 genes utilised for molecular subtyping from TCGA [7]. A predictive model based on the TCGA samples was trained using support vector machine (SVM) algorithm for molecular subtype classification. Then, this model was applied for each sample in the remaining 12 datasets. The SVM model was built using the 'e1071' package in R. The Cramer's V coefficient of the paired molecular subtype was calculated to evaluate the concordance between the subtypes predicted by our SVM model and those reported by Verhaak et al. [23]. The value of Cramer's V statistic index was between zero and one. The values ranging from 0.36 to 0.5 suggested substantially correlated relationship, and values larger than 0.5 indicated a closely correlated result. Detailed information on the distributions of molecular subtypes and clinical information for each study are listed in Table S3.

### 2.3. Estimated fractions of the infiltrating immune cells from gene expression profiles

CIBERSORT is a deconvolution algorithm that utilises a set of reference gene expression values as a minimal representation for each cell type and estimates the cell composition of complex tissues on the basis of the gene expression profiles from bulk tumour samples with support vector regression [22]. The leucocyte gene signature matrix, termed LM22, with 547 genes can be used to distinguish 22 human haematopoietic cell phenotypes, including naive and memory B cells, seven T cell types, natural killer cells, macrophages, plasma cells, dendritic cells, eosinophils, myeloid subsets and neutrophils. The detailed definition of these 22 immune cell subsets can be found from Table S2 of Newman's publication [22]. The LM22 signature matrix and the CIBERSORT R function at 1000 permutations were explored to quantify the relative proportions of 22 subsets of tumour-infiltrating immune cells by using the normalised gene expression data prepared with the standard annotation files. For each sample, an empirically defined global p-value, which measures the confidence of the results for the deconvolution, was determined. The inference of the proportions of immune cells was performed separately in each dataset used in this study. In addition, the total of all 22 estimated immune cell type proportions was one for each sample. Pairwise correlations between the immune cell subtypes for the pooled cohort and within different molecular subtypes were

estimated using the Pearson's correlation coefficient depicted in heatmaps.

Another measurement of immune infiltration, as proposed by Rooney et al. [24], represented the geometric mean value of *PRF1* and *GZMA*. This index was calculated for the TCGA HGSOC and Tothill dataset.

### 2.4. Statistical analyses

Information on age, tumour histotype, grade, treatment regimen and survival were collected. The clinical endpoints were progression-free survival (PFS) and OS. PFS was defined as the interval between the date of diagnosis until the date of development of distance metastasis or relapse. OS was defined as the length of time between the date of diagnosis until the date of death from any cause. The detailed type of survival time provided by the contributor of each study is recorded in Table S1.

Given that monocytes are primarily in circulation and become macrophages upon extravasation, they were excluded from the association analysis. Survival analysis was performed to test the associations between the 21 immune cell fractions and the survival in the whole cohort and by molecular subtype. Samples with a follow up time or survival time of less than 1 month or with a CIBERSORT p value $\geq$ 0.05 were excluded from the survival analysis. In the Cox proportional hazard models, quartiles (25%, 50% and 75%) of the relative proportion (ranging from zero to one) of each of the 21 immune cell subsets were calculated and treated as continuous variables. Quartiles were calculated overall and by molecular subtype within each dataset. The immune cell subtypes, which were statistically significantly associated with survival [p value derived by test with null hypothesis of the hazard ratio (HR) equal to one $<$ 0.05] in the unadjusted univariate Cox proportional hazard model, were selected in the multivariable Cox proportional hazard models. The covariate histological grade and the Figo stage were included in multivariable analyses for adjustment. The log-rank p value was calculated to evaluate the differences in the survival rate between groups, and the respective survival curves based on the Kaplan–Meier estimation were delineated. Survival analysis was also performed between the immune cell subsets with survival within each dataset. The associations between the immune checkpoints (PD1, PDL-1, PDL-2 and CTLA4) and survival were tested using the methods described above.

Furthermore, the problem that the exclusion of important variables is possibly correlated with prognosis when confounding factors are controlled may arise when a variable from univariate analysis was selected [25]. To address this concern, the multivariable Cox proportional hazard models (with 23 variables that are the 21 immune cell types, stage and grade) were fitted via the penalised maximum likelihood with the R package 'glmnet' [26]. The penalisation factor was chosen depending on the result of 1000 cross-validation tests.

To explore whether distinct patterns of HGSOC tumour-infiltrating immune cells exist and whether these patterns are associated with the survival of patients with HGSOC after platinum-based chemotherapy, hierarchical clustering of immune cell fractions was conducted in patients with a CIBERSORT p value $<$ 0.05. To provide comparability between the abundant (high overall ratio) and rare (low overall ratio) immune cell subsets, the relative cell proportion values were scaled between 0 (the observed smallest value) and 1 (the observed greatest value) for each immune cell type.

Hierarchical clustering of the rescaled data was conducted by partitioning around the medoid (PAM) algorithm with the 'fpc' R package across all HGSOC samples included in this study. The average silhouette width was utilised to determine the number of distinct subtypes. The association between tumour immune cell infiltration clusters and survival were evaluated using the statistical methods described above.

All analyses in this study were performed using the R software (version 3.3.3) [27]. Results were considered statistically significant when $p < 0.05$, and all the statistical tests performed were two-sided. Researchers who wish to access the R codes may send a request email to the corresponding author, Rong Liu (liuronghyw@csu.edu.cn).

## 3. Results

### 3.1. Performance of the SVM prediction model for subtypes across different studies

An SVM-based predictive model for molecular subtype classification was trained in TCGA discovery samples ($n$ = 488) by using 100 marker genes from the study of Verhaak et al. [7]. Each sample in the remaining 12 datasets was classified into one of the four subtypes: 'Differentiated', 'Mesenchymal', 'Immunoreactive' and 'Proliferative'. Ten TCGA expression profiles not included in the discovery dataset and 422 expression profiles with molecular subtypes predicted by Verhaak et al. [7] from three published studies were analysed to verify the classification power of the SVM model. The Cramer's V coefficients of the paired prediction overlap for TCGA discovery dataset, TCGA validating dataset, Tothill, BONOME and Yoshihara_1 were 0.991, 0.894, 0.793, 0.755 and 0.857, respectively, suggesting high concordance (Table S4). Survival analysis by using the whole dataset revealed a highly significant difference in OS (log rank $p < 1 \times 10^{-3}$, Fig. S1a) and PFS (log rank $p$ = 0.052, Fig. S1b) amongst the four molecular subtypes. The prognosis of patients within the immunoreactive subtype was the best amongst these four subtypes, which was consistent with the finding of Verhaak et al. [2].

### 3.2. Tumour-immune infiltration evaluated using the CIBERSORT across studies

Fig. 2a summarises the tumour-immune infiltration of the 2218 HGSOC samples. The gene expression profiles of the 13 studies were measured using eight types of microarray-based platforms (Table S1). The ratio of the 547 genes, included in the LM22 signature matrix available for the CIBERSORT analysis, was also calculated (Fig. S2). The average value of the represented proportion of genes was 91.1% (gene numbers ranging from 432 to 517). The least and most variable cell types of the samples across different studies were the neutrophils [mean = 1.4%, standard deviation (SD) = 2.3%] and the M0 macrophages (mean = 10.5%, SD = 11.8%), respectively. The following analyses were restricted to samples with an empirical p value derived by the CIBERSORT with Monte Carlo sampling less than 0.05 unless otherwise specified. Ali et al. reported that this p value reflects the overall proportion of immune cells in breast tumours, wherein a large ratio of tumour-infiltrating immune cells corresponds to a small p value [12]. Their finding was validated in the HGSOC samples. A metric of immune cytolytic activity has been defined as the geometric mean of *GZMA* and *PRF1* expression by Rooney et al. [24] The cytolytic activities for TCGA and Tothill dataset were also calculated, and results revealed strong ordinal relationships between the cytolytic activities and the CIBERSORT p value cutoffs (one-way ANOVA p value $< 2 \times 10^{-16}$, Fig. 2b–c). Furthermore, the p value thresholds were associated with the patients' OS. Fig. 2d depicted that the $p < 0.01$ subgroup, which corresponded to the greatest proportion of tumour-infiltrating immune cells amongst these three subtypes, was associated with significantly improved OS [HR = 0.77, 95% confidence interval (CI) = 0.68–0.87; $p = 3.19 \times 10^{-5}$] compared with the $p \geq 0.05$ group, whereas a $0.01 \leq p < 0.05$ presented an intermediate OS significantly different with that of the $p \geq 0.05$ group (HR = 0.81, 95% CI = 0.70–0.94; $p = 6.02 \times 10^{-3}$). This result supported that the empirical CIBERSORT p value reflected the ratio of immune cells to nonimmune cells.

Pairwise correlation relationships between the ratios of 22 different immune cells infiltrated in tumour for the pooled population

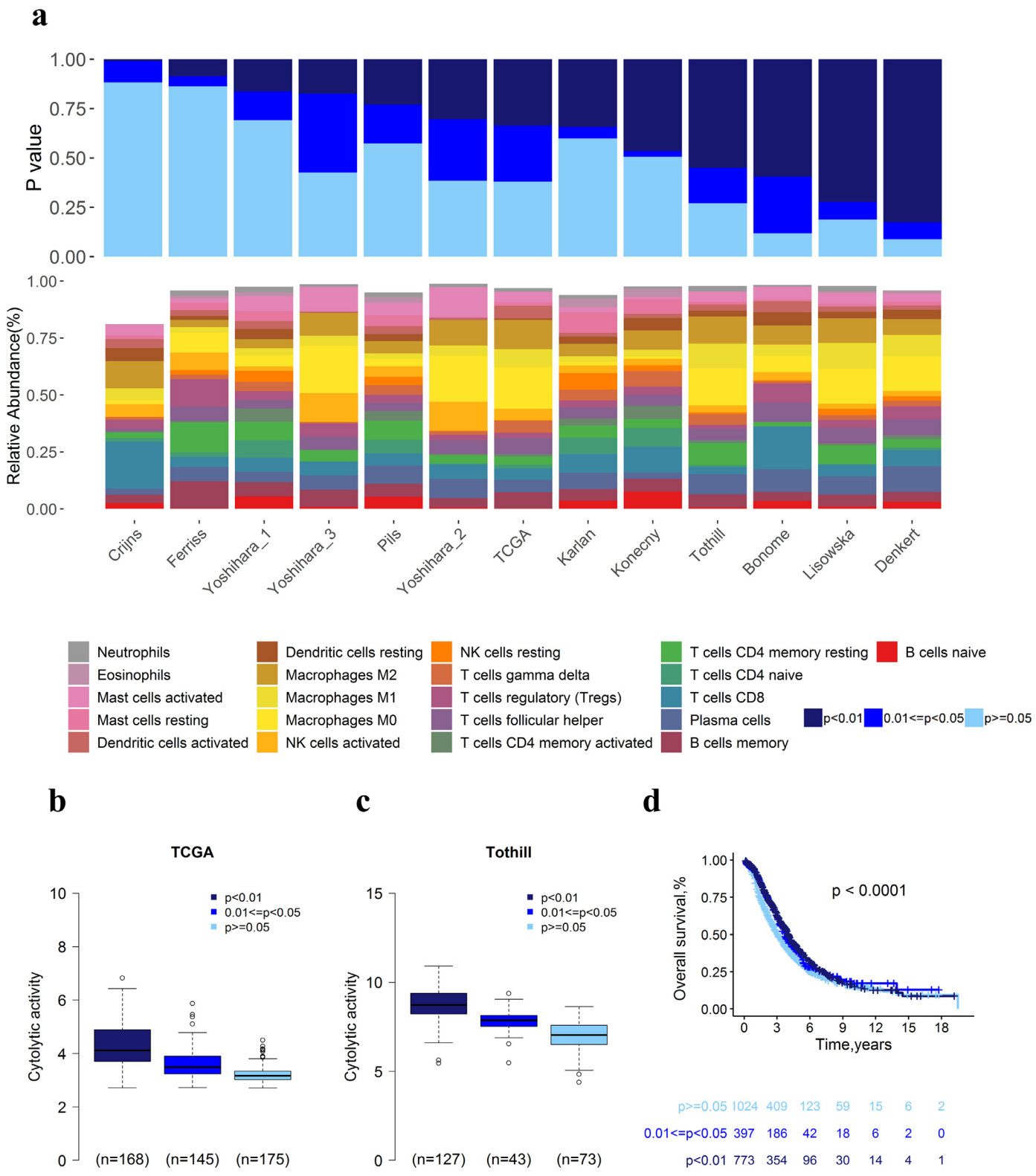


**Fig. 2. Summary of inferred 21 tumour-infiltrating immune cell subset strata by study.** (A) Bar charts summarising immune cell subtype fractions against empirical CIBERSORT p-value distributions by study. Box plots describing the association between immune cytolytic activity and CIBERSORT p-value in TCGA (b) and Tothill (c) datasets; (d) Survival curves based on Kaplan–Meier estimation of groups defined by CIBERSORT p-value (p-value depicted in the picture is from log-rank tests). NK cells, natural killer cells; TCGA, The Cancer Genome Atlas.

were weakly to moderately correlated overall (Fig. S3) and in four different molecular subtypes (Figs. S4–S7). Overall, CD8+ T cells and resting dendritic cells represented the strongest positive correlation (Pearson's correlation coefficient = 0.28), whereas the M0 macrophages and CD8+ T cells represented the strongest negative correlation (Pearson's correlation coefficient = −0.42). Broadly, the patterns of correlation between the different tumour infiltrating immune cell subsets were similar regardless of molecular subtype.

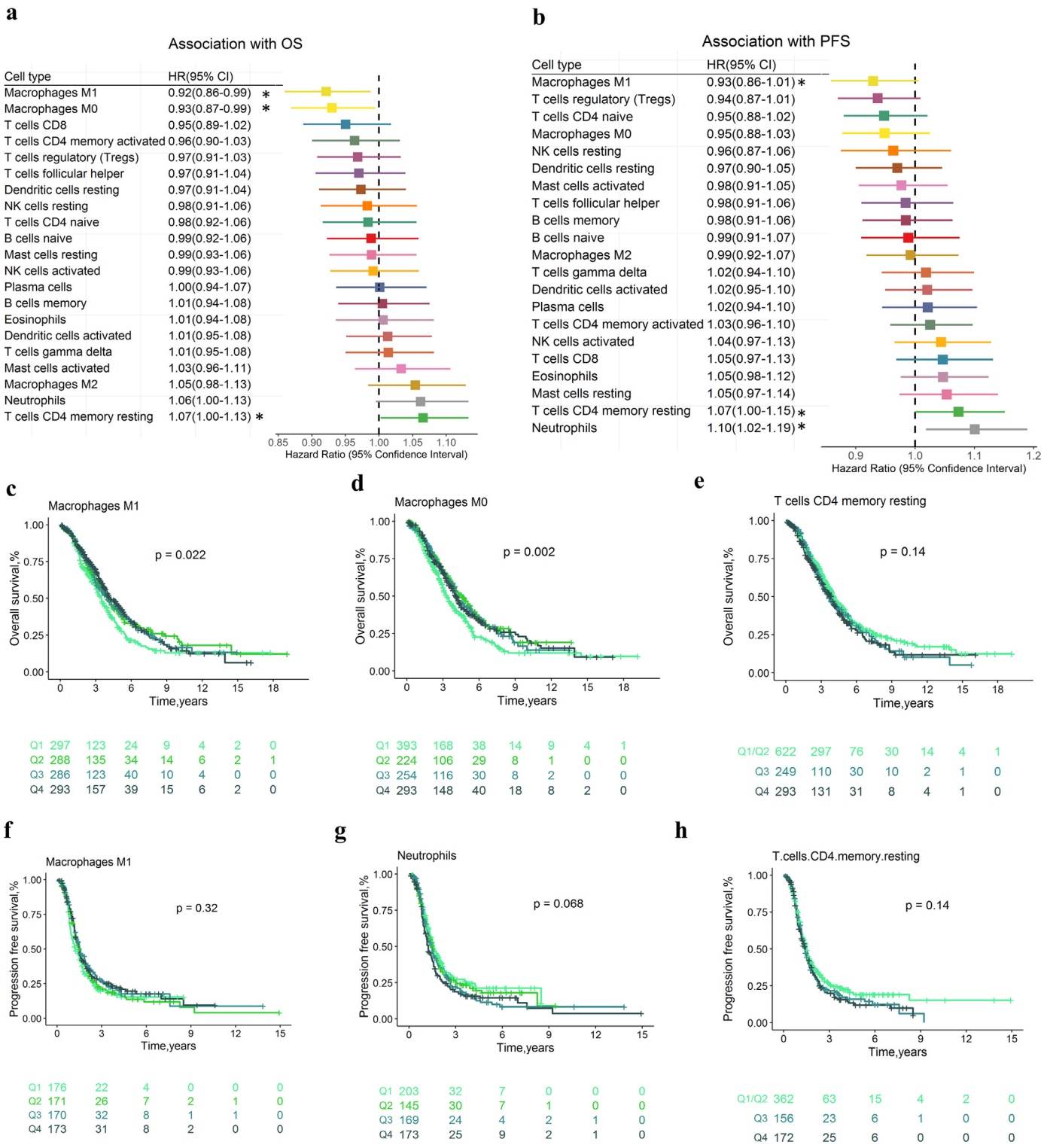


**Fig. 3. Associations between survival and immune cells in the whole cohort.** Survival analysis was limited to samples with CIBERSORT p-value < 0.05. Unadjusted HRs (boxes) and 95% confidence intervals (horizontal lines) for immune cell subsets associated with OS (a) and PFS (b) are shown. Box size is proportional to the standard error of HR and inversely proportional to the width of the confidence interval. Asterisks indicate HRs with a p value (testing the null hypothesis that HR is equal to one) < 0.05. Survival plots of quartiles of statistically significant immune cell subsets (q-value < 0.05, c–h). Depicted p-values are from log-rank tests. HR, hazard ratio.

### 3.3. *Prognostic effect of immune cell subsets*

The immune cell type fractions were associated with survival of HGSOC treated with platinum chemotherapy. The unadjusted HRs and corresponding 95% CIs for the quartiles of immune cell type fraction for OS and PFS are depicted Fig. 3a and b, respectively. After filtering the samples with CIBERSORT $p \geq 0.05$, 1164 HGSOC cases were noted with a median OS of 2.83 years (649 events), with the type of prognosis being PFS for 690 cases (median PFS time was 1.25, 502 events). In general, the resting CD4+ memory T cells were associated with poor OS (HR = 1.07, 95% CI = 1.00–1.13; $p = 0.04$) and PFS (HR = 1.17, 95% CI = 1.00–1.15; $p = 0.05$). Neutrophils were associated

with PFS (HR = 1.10, 95% CI = 1.02−1.19; $p = 1.53 \times 10^{-2}$). Of these results, neutrophils can potentiate or oppose cancer progression depending on the signals originating from stromal or cancer cells within the tumour microenvironment [28]. The M0 (HR = 0.93, 95% CI = 0.87−0.99; $p = 0.03$) and the M1 (HR = 0.92, 95% CI = 0.86−0.99; $p = 0.02$) macrophages were correlated with favourable OS. Their association with OS in separate datasets utilised in this study is shown in Fig. S8. The high density of M1 macrophages had been associated with a favourable prognosis amongst patients with ovarian, gastric and non-small-cell lung cancers or hepatocellular carcinoma [29]. Multivariable analyses adjusted for prognostic covariates (stage and grade) were then conducted, and results revealed that the M0 macrophages (HR = 0.94, 95% CI = 0.87−1.01; $p = 0.07$) contributed to the model for OS (Table S5a). As for PFS, the neutrophils (HR = 1.10, 95% CI = 1.01−1.18; $p = 0.02$) and the resting CD4+ memory T cells (HR = 1.08, 95% CI = 1.00−1.15; $p = 3.87 \times 10^{-2}$) contributed to the model (Table S5b). Their associations with PFS in separate cohorts are depicted in Fig. S9. Neutrophils are previously reported to be associated with OS and treatment response in breast cancer based on CIBERSORT analysis [12,30]. The multivariable Cox proportional hazard models for OS and PFS with penalised maximum likelihood estimation are shown in Tables S5c and S5d, respectively.

### 3.4. Variation of the association between immune cell fractions and prognosis by molecular subtype

The prognostic value of the 21 immune cell proportions was evaluated according to the four molecular subgroups of HGSOC. Variations in the prognostic effect of different immune cells by molecular subtype were found.

In the differential subpopulation, the CD8+ T cells (HR = 1.17, 95% CI = 1.00−1.37; $p = 0.04$) and the resting mast cells (HR = 0.85, 95% CI = 0.73−0.99; $p = 0.04$) showed association with OS (Fig. 4a), and none of the 21 immune cell proportions displayed a significant association with PFS (Fig. 5a) in univariate analyses. Multivariable survival analyses adjusted for stage and grade revealed that no immune cell fraction contributed to the model for OS (Table S5E). Given that none of the immune cell proportion was significantly associated with PFS with normal p value $< 0.05$, the multivariable survival analysis adjusted for clinical factors for PFS was not conducted. Furthermore, the multivariable Cox proportional hazard model with penalised maximum likelihood estimation suggested that the CD8+ *T* cells (HR = 1.05), M2 macrophages (HR = 1.05), activated dendritic cells (HR = 1.09) and neutrophils (HR = 1.07) contributed to the model for OS (Table S5F), whereas no immune cell proportion contributed to the model for OS (Table S5G).

In the immunoreactive subpopulation (Fig. 4b), the CD8+ T cells (HR = 0.86, 95% CI = 0.76−0.96; $p = 8.82 \times 10^{-3}$, Fig. 4e) and the M0 macrophages (HR = 0.85, 95% CI = 0.76−0.95; $p = 3.40 \times 10^{-3}$, Fig. 4f) were associated with good OS. The M2 macrophages (HR = 1.18, 95% CI = 1.05−1.33; $p = 4.85 \times 10^{-3}$) were associated with poor OS. The associations between these three immune cells in different cohorts are shown in Fig. S10. In multivariate analysis adjusted for known prognostic factors (Table S5H), the M0 macrophages (HR = 0.87, 95% CI = 0.77−0.99; $p = 0.03$) and the CD8+ T cells (HR = 0.85, 95% CI = 0.74−0.96; $p = 0.01$) contributed to the model for OS. The CD8+ T cells had the smallest HR and the most significant p value. None of the immune cell proportions were associated with PFS in the univariate (Fig. 5b) and multivariate (Table S5J) analysis models. The CD8+ T cells were associated with the lowest HR point estimates in OS (HR = 0.93) in the multivariable Cox proportional hazard models with penalised maximum likelihood estimation.

In the mesenchymal subtypes, the resting dendritic cells were associated with OS (HR = 0.85, 95% CI = 0.73−0.97; $p = 1.96 \times 10^{-2}$; Fig. 4c), the M1 macrophages were associated with PFS (HR = 0.83, 95% CI = 0.71−0.97; $p = 1.88 \times 10^{-2}$), and a high level of neutrophils were associated with worse PFS (HR = 1.18, 95% CI = 1.01−1.37, $p = 3.49 \times 10^{-2}$) (Fig. 5c). Multivariable analyses adjusted for grade and stage showed that none of the immune cell proportions was associated with OS (Table S5K), whereas the M1 macrophages (HR = 0.79, 95% CI = 0.68−0.92; $p = 1.99 \times 10^{-3}$) contributed to the model for PFS (Table S5L) and were associated with the lowest HR point estimate in PFS (HR = 0.89, Table S5N).

In the proliferative subpopulations, the eosinophils were associated with OS (HR = 1.26, 95% CI = 1.03−1.54, $p = 2.60 \times 10^{-2}$, Fig. 4d) in univariate analysis. Multivariate analysis showed that the eosinophils (HR = 1.23, 95% CI = 1.02−1.47, $p = 2.72 \times 10^{-2}$) contributed to the model for OS (Table S5O). Table S5P depicts the multivariable Cox proportional hazard model for OS with penalised maximum likelihood estimation. Eosinophils were associated with the highest HR point estimates (HR = 1.15). The activated CD4 + memory T cells (HR = 1.27, 95% CI = 1.04−1.55; $p = 1.64 \times 10^{-2}$), T cell gamma delta (HR = 1.49, 95% CI = 1.18−1.89; $p = 8.38 \times 10^{-4}$), eosinophils (HR = 1.25, 95% CI = 1.03−1.53, $p = 2.72 \times 10^{-2}$) and resting mast cells (HR = 1.26, 95% CI = 1.02−1.54; $p = 3.11 \times 10^{-2}$) were associated with poor PFS, whereas the activated mast cells (HR = 0.78, 95% CI = 0.63−0.98; $p = 3.29 \times 10^{-2}$) were associated with favourable PFS (Fig. 5e). The eosinophils (HR = 1.34, 95% CI = 1.09−1.65; $p = 5.98 \times 10^{-3}$) and the activated CD4+ memory T cells (HR = 1.36, 95% CI = 1.11−1.66; $p = 2.85 \times 10^{-3}$) remained significantly associated with PFS in the multivariate model adjusted for known clinical factors (Table S5Q). In the multivariable Cox proportional hazard model for PFS with penalised maximum likelihood estimation, the activated CD4+ memory T cells, eosinophils, and resting mast cells showed large HR point estimates (HR $> 1.1$, Table S5R).

### 3.5. Immune clusters associated with survival, molecular subtype and stage

Based on the immune cell fractions of samples with CIBERSORT p value $< 0.05$, hierarchical clustering was performed to explore whether distinct patterns of tumour immune cell infiltration can be identified. The average silhouette width index of the PAM algorithm was interpreted to suggest five clusters in the pooled cohort (Fig. S11). The tumour immune cell proportions by these four clusters are shown in Fig. 6a, and boxplots depict their distributions (Figs. S12−S13). Distinct patterns of OS (Fig. 6b) and PFS (Fig. 6c) were found between different immune clusters. Cluster 4, which had high levels of activated mast and natural killer cells and low level of resting mast cells, was associated with favourable prognosis. By contrast, cluster 3, defined by low levels of M0 macrophages and CD8+ T cells and high levels of M2 macrophages, was associated with poor OS. Cluster 1 displayed low levels of CD8+ T and activated memory CD4+ T cells and high levels of M1 macrophages. Cluster 2 had high levels of CD8+ T, gamma delta T and activated CD4 memory cells and low levels of resting CD4+ memory cells. Meanwhile, cluster 5 had high expression levels of naïve B cells and low expression levels of M0 and M1 macrophages.

The immune clusters were significantly associated with the molecular subtype (p value of chi-square test = $3.12 \times 10^{-10}$, Fig. S14a). This relationship was mainly observed in cluster 2, which was especially enriched with the immunoreactive subtype (56.4% to 40.4% overall). Immune clusters were also significantly associated with tumour grade ($p = 1.55 \times 10^{-12}$, Fig. S14b). Cluster 4 had no grade 4 tumours and was enriched with grade 2 tumours (35.0% to 19.3% overall). No significant association was observed between the immune cluster and patient's stage (p value of chi-square test = 0.102, Fig. S14c) and age (p value of one-way ANOVA = 0.923, Fig. S14d). Collectively, these findings suggested that considerable variability existed in the nature of the tumour immune infiltrate across different HGSOC tumours, partly

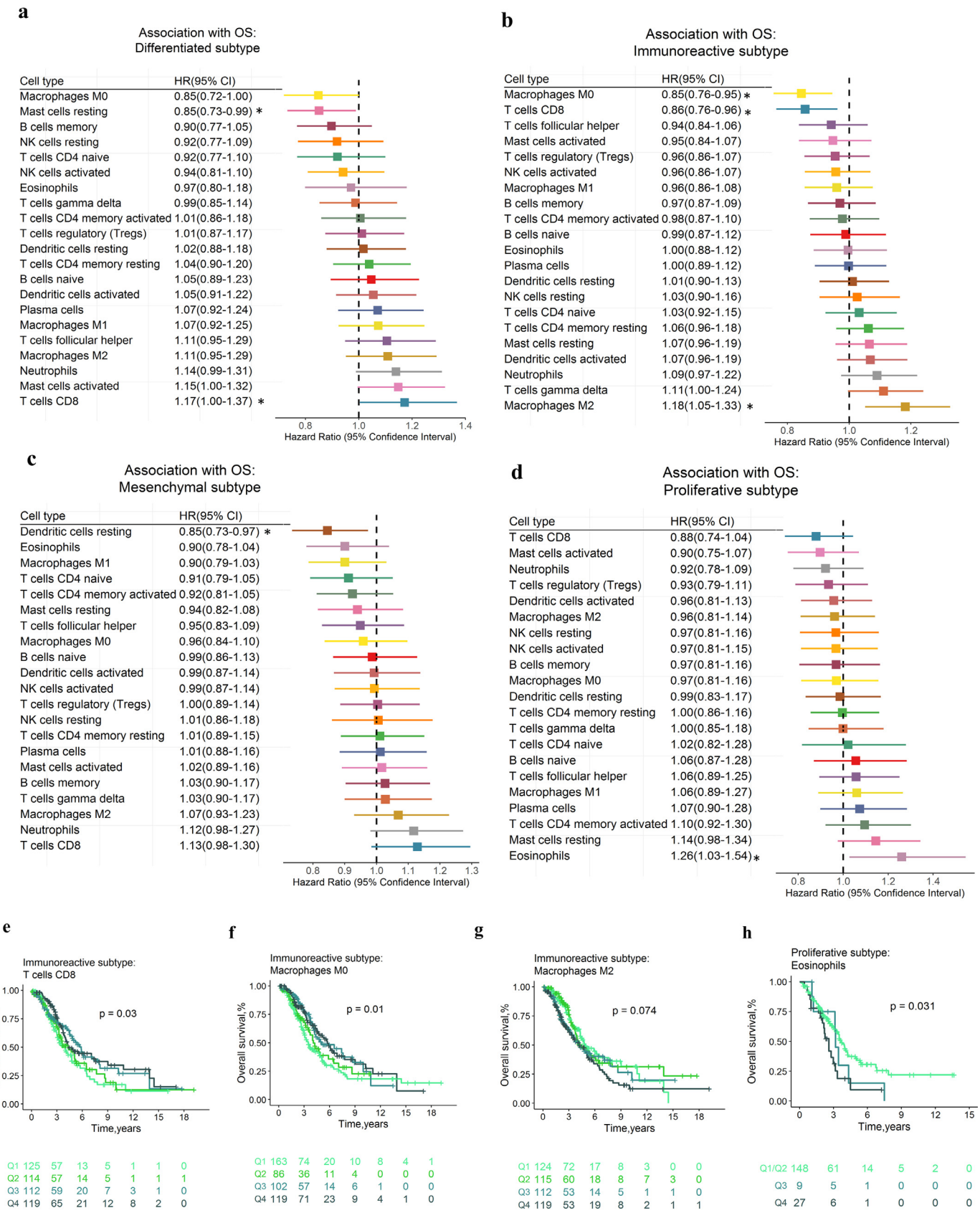


**Fig. 4. Associations between OS and immune cells by molecular subtype.** Unadjusted HRs (boxes) and 95% confidence intervals (horizontal lines) limited to samples with CIBERSORT p-value < 0.05 for the association with OS in four molecular subtypes (a–d). Box size is proportional to the standard error of HR and inversely proportional to the width of the confidence interval. Asterisks denote a p-value (testing the null hypothesis that HR is equal to one) < 0.05. Survival plots of quartiles of immune cell subsets (e–h). Depicted p-values are from log-rank tests. HR, hazard ratio. OS, overall survival.

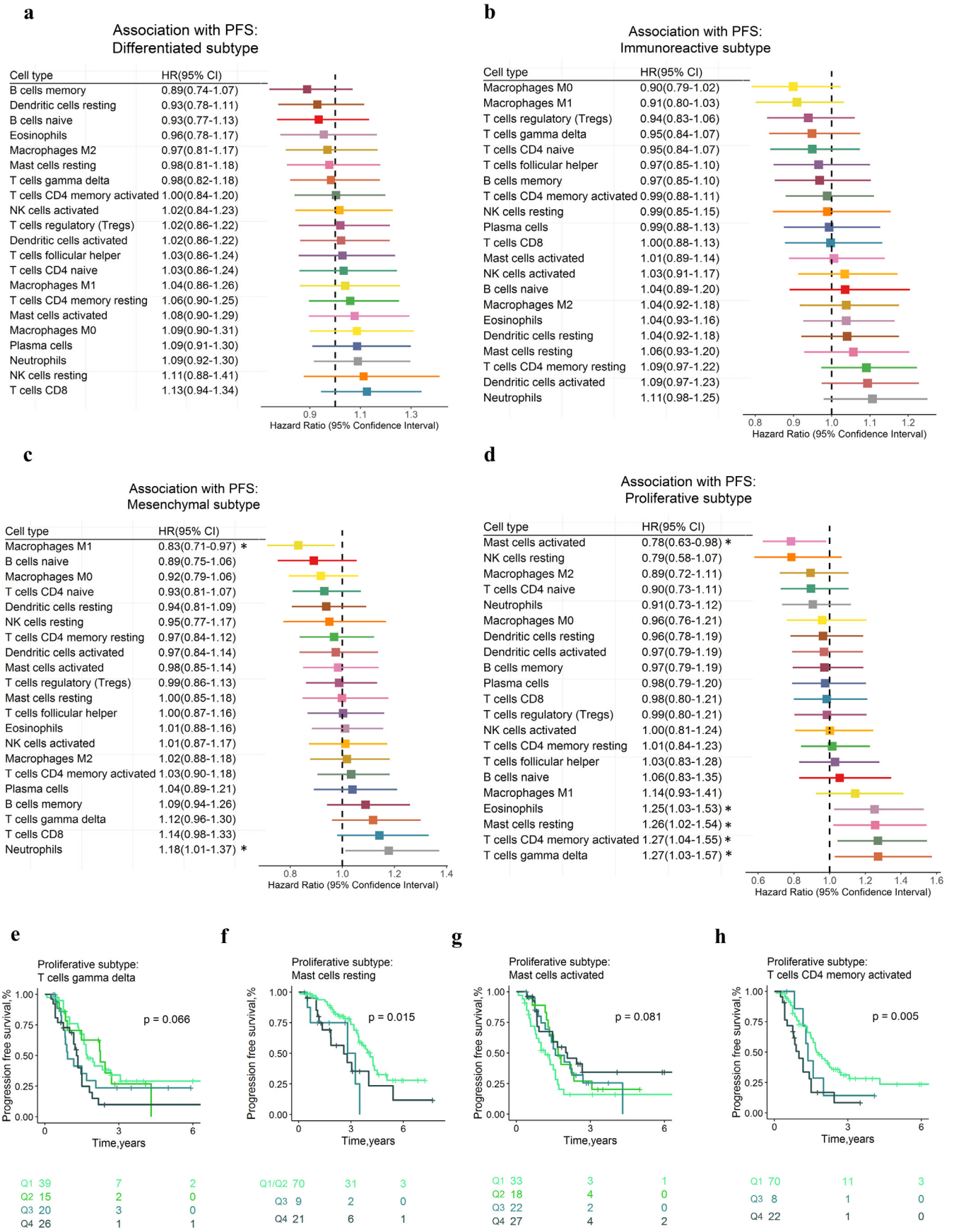


**Fig. 5. Associations between PFS and immune cells by molecular subtype.** Unadjusted HRs (boxes) and 95% confidence intervals (horizontal lines) limited to samples with CIBERSORT p-value < 0.05 for the association with PFS in four molecular subtypes (a–d). Box size is proportional to the standard error of HR and inversely proportional to the width of the confidence interval. Asterisks denote a p-value (testing the null hypothesis that HR is equal to one) < 0.05. Survival plots of quartiles of immune cell subsets (e–h). Depicted p-values are from log-rank tests. HR, hazard ratio; PFS, progression-free survival.

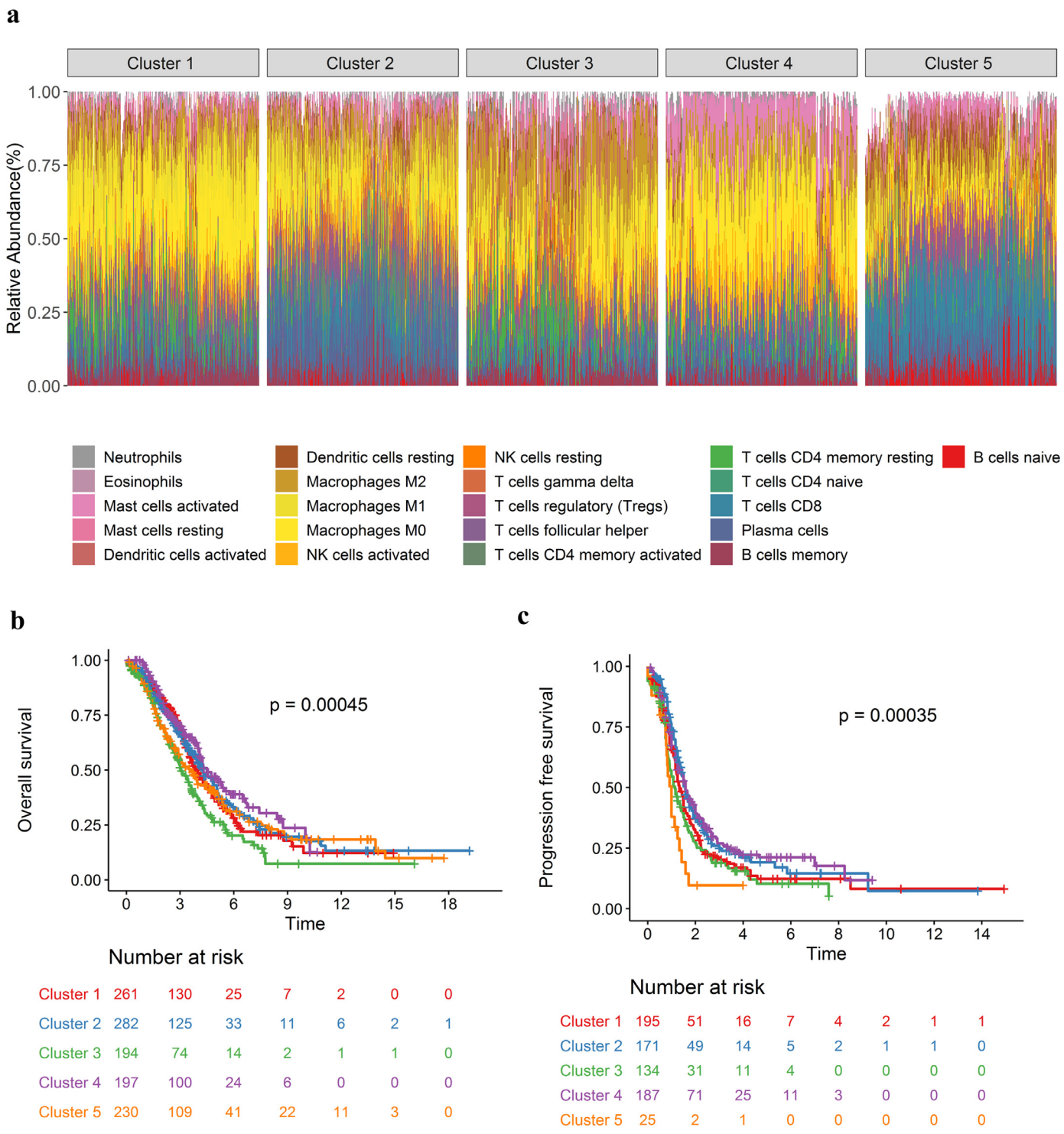


**Fig. 6. Hierarchical clustering of all samples based on immune cell proportions and survival plots by clusters.** Stacked bar charts of samples ordered by cluster assignment (a). Survival plots for OS (b) and PFS (c) by cluster. Variables are stratified as quartiles for the plots. Depicted p-values are from log-rank tests.

accounting for molecular features of the tumour. Thus, this condition may affect the prognosis of patients, who underwent platinum-based treatment.

### 3.6. Immune checkpoint targets are prognostic

The immune checkpoint molecules that are targets of clinically utilised drugs (anti-CTLA-4, anti-PD-1 and anti-PD-L1) were investigated for associations with survival of patients with HGSOC (Table S6). Pairwise correlation relationships between the expressions of PD1, PD-L1, PD-L2 and CTLA4 for the pooled population were highly correlated (Pearson's correlation coefficients $\geq$ 0.39, Fig. S15). High expression levels of CTLA-4 were associated with improved OS (HR = 0.92, 95% CI = 0.88–0.96; $p = 5.50 \times 10^{-4}$, Fig. 7a), and high PD1 was correlated with good PFS (HR = 0.94, 95% CI = 0.89–1.00; $p = 4.51 \times 10^{-2}$, Fig. 7b) within the combined whole dataset. These results were consistent with the finding of Darb-Esfahani et al. that high PD-1 and PD-L1 levels are indicators of a favourable prognosis

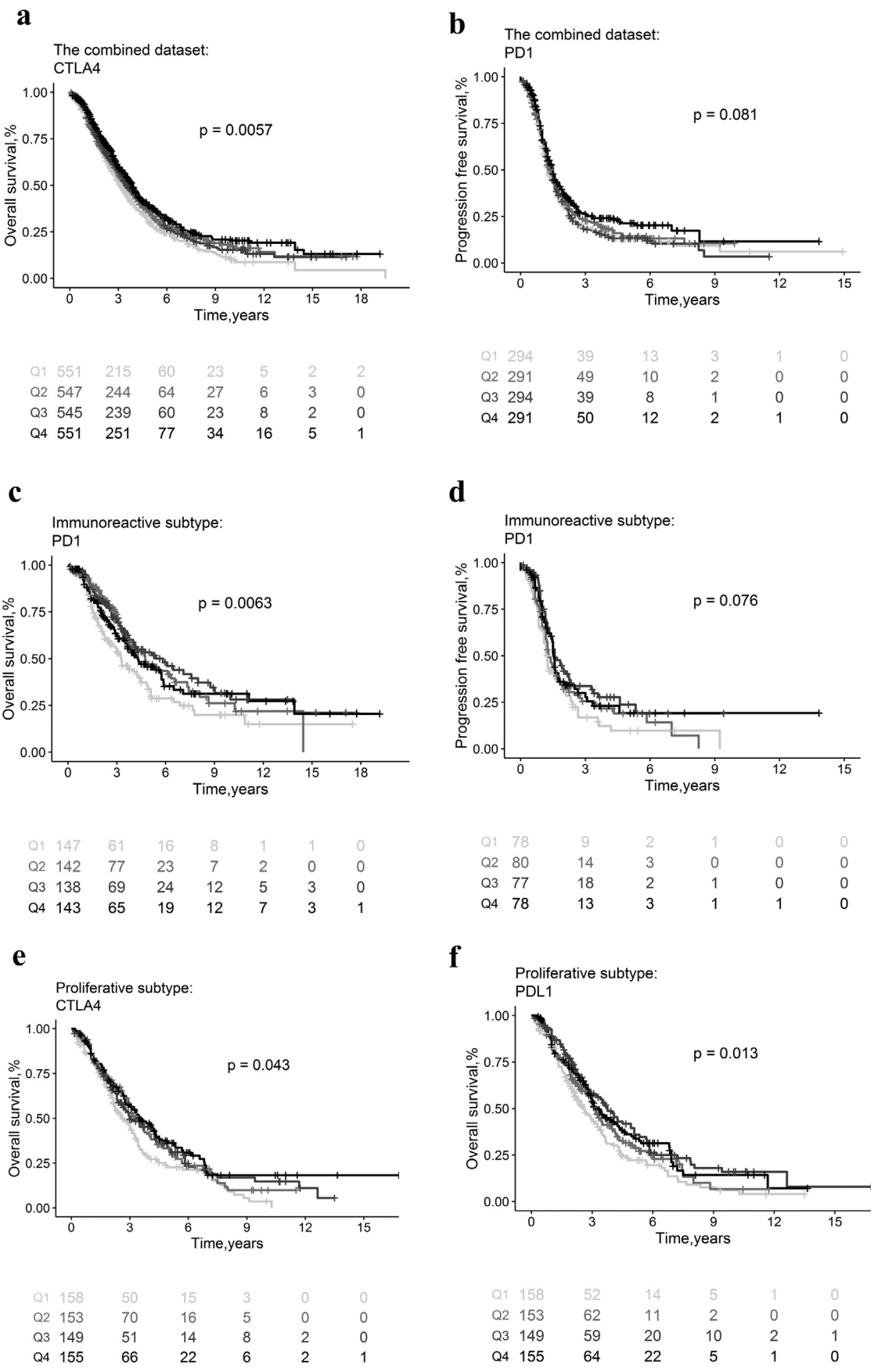


**Fig. 7. Kaplan–Meier curves showing the association of immune checkpoint molecules and clinical outcomes.** Associations of CTLA-4 (a) and PD1 (b) with overall survival in the combined whole dataset with 2218 patients with HGSOC. Associations of PD-1 with overall survival (c) and PFS (d) within immunoreactive subtype. Associations of CTLA-4 (e) and PD-L1 (f) with OS within proliferative subtype. Variables are stratified as quartiles for the plots. Depicted p-values are from log-rank tests.

in HGSOC [31]. In the immunoreactive subtype, PD1 was associated with favourable OS (HR = 0.89, 95% CI = 0.80−1.00; $p = 4.32 \times 10^{-2}$, Fig. 7c) and PFS (HR = 0.89, 95% CI = 0.79−1.01, $p = 6.66 \times 10^{-2}$, Fig. 7d). In the proliferative subtype, CTLA-4 (HR = 0.88, 95% CI = 0.80−0.96; $p = 6.06 \times 10^{-3}$, Fig. 7e) and PDL-1 (HR = 0.88, 95% CI = 0.81−0.97; $p = 8.29 \times 10^{-3}$, Fig. 7f) were associated with good OS. Webb et al. found that the PD-L1 expression is correlated with tumour-infiltrating T cells and favourable prognosis in HGSOC [32].

## 4. Discussion

In this study, the relative proportions of 22 immune cell phenotypes in a large dataset of patients with HGSOC ($n = 2218$) were estimated using deconvolution algorithm based on gene expression data from bulk tumour tissue. The positive association between tumour immune cell infiltration with M1 macrophages and good prognosis and the negative association between neutrophils and poor prognosis were confirmed. High levels of CD8+ T cells and PD1 expression were correlated with favourable OS in the immunoreactive subtype. Differences exist in the cellular composition of the immune infiltrate in HGSOC tumours and may be critical determinants of survival after platinum chemotherapy within molecular subtypes.

Large public repositories of gene expression data on a genomic scale established over the past 20 years were reinvigorated by the advances in computational techniques, providing an opportunity to reanalyse the gene expression data from multiple studies. A comprehensive association analysis was performed between the survival and the tumour immune cell infiltrations in HGSOC by inferring the fractions of 22 immune cell types from tumour transcriptomes by using CIBERSORT [22]. The methods developed for genome data informed cell type quantification include CIBERSORT, xCell [33], TRUST (which was designed for RNA-seq data) [34] and a recently published algorithm, FARDEEP (Fast And Robust DEconvolution of Expression Profiles), that can provide the absolute cell abundance estimation [35]. Although the algorithms utilised in the abovementioned methods were different, they were developed for the same purpose. Given that no objective comparison exists between these methods regarding the accuracy of estimation, the most widely used [12,30,36] and robust method was selected by us.

Overall, increased proportion of estimated immune cell infiltrations was associated with favourable OS. This result supported the finding of a meta-analysis of 10 independent studies with 1815 patients that the lack of intraepithelial lymphocytes was significantly associated with poor prognosis in patients with ovarian cancer [21]. Of the cell subtypes investigated, the M1 and M0 macrophages were associated with improved survival. Tumours at all stages possibly contained particular abundant macrophages in diverse states. The M1 and M2 states were polarised from the M0 states. High fractions of M1 and M0 macrophages were associated with good prognosis. The distinct immunoregulatory functions of activated M1 and M2 macrophages are antitumoural and protumoural, respectively [37]. As reported, the M1 macrophages are highly potent against tumours and positively correlated with survival in HGSOC [38]. In addition, the fractions of macrophages contributed to the definition of immune subgroups in unsupervised hierarchical clustering analysis with prognostic implications. Previous clinical studies and experimental mouse models suggested that macrophages are protumoural and immunosuppressive [11]. In this study, the diversity of macrophages' functional status was highlighted, rather than treating macrophages in a variety of status equally. This point is of critical importance for treatments to combat the tumour-promoting roles of macrophages in early clinical trials [39]. In this study, the neutrophils were found to be associated with poor prognosis for HGSOCs. Emerging evidence suggests that tumours manipulating neutrophils can create diverse phenotypic and functional polarisation states that can change tumour behaviour associated with cancer progression [28]. Divergent phenotypes, depending on specific tumour-derived factors, were caused by neutrophil polarisation. G-CSF, transforming growth factor-$\beta$ and interferon-$\beta$ are the typical molecules in this process. In general, the activation of transforming growth factor-$\beta$ and G-CSF can activate a tumour and a metastasis-promoting biological process [40]. Meanwhile, IFN$\beta$ acts as a negative regulator of the protumourigenic phenotype of neutrophils [41].

Differences were observed in molecular subtypes regarding immune cell fractions associated with survival after platinum-based chemotherapy. Estimated high levels of M0 macrophages and CD8+ T cells and low levels of M2 macrophages were associated with favourable OS in HGSOCs within the immunoreactive subtype. The main function of CD8+ T cells is to protect against intracellular pathogens and tumour [42]. They can gradually deteriorate T cell function, a state called exhausted T cells, when exposed to excessive amount of antigen and/or inflammatory signals [43]. Exhausted T cells are one of the main reasons for the failure of immune checkpoint inhibitor therapy because the characteristic of exhausted T cells is progressive loss of effector functions (killing and cytokine production function) and expression of multiple inhibitory receptors [44]. Notably, the levels (negative, low, moderate and high) of tumour-infiltrated CD8+ T cells in the HGSOC tumours revealed positive correlation with the patients' survival regardless of the extent of residual disease, therapy or BRCA1 mutation [45].

Amongst the proliferative subtypes, the high levels of gamma delta T, resting mast and activated CD4+ memory T cells and the low level of activated mast cells were associated with poor PFS. The gamma delta T cells involved in the initiation and propagation of immune responses can play protective roles in cancer, largely accounting for their potent cytotoxicity and interferon-$\gamma$ production [46]. As revealed in a pan-cancer study conducted by Gentles et al., the gamma delta T cell signature is associated with favourable prognosis [30]. This finding was in contradiction with that in the proliferative subtype, as only 100 samples were available within the proliferative subtype to test the association between PFS and immune cell subsets. The function of gamma delta T, mast and CD4+ memory T cells in platinum resistance within this subtype needs further biological exploration.

The unsupervised hierarchical clustering analysis based on immune cell proportions revealed four distinctive immunologic subgroups of HGSOC. Trying to include specific types of HGSOC in clinical evaluations of immunomodulatory agents may be worthwhile. Such actions may be able to alter the immune infiltration patterns shown in our clustering analysis and increase response to platinum-based chemotherapy.

To understand whether the immune system participates in the prognosis of ovarian cancer, genomic data or in situ histological analysis was utilised to measure the immune cell infiltrations in previous immune profiling studies [19−21,47,48]. Patients with increased frequencies of intraepithelial CD8+ tumour-infiltrating lymphocyte are correlated with improved survival amongst patients with ovarian cancer [19,21]. Moreover, 73.9% of patients with pre-existing tumour-associated/infiltrated lymphocytes have complete response after platinum-based chemotherapy, whereas only 11.9% patients without tumour-associated/infiltrated lymphocytes have reached complete response [20]. A recent study on in situ histological analyses found that mature dendritic cells are associated with favourable immune infiltrate and improved prognosis in patients with ovarian cancer [47]. These approaches supported the prognostic significance of the tumour infiltration by lymphocytes but had the limitation of only one or two immune cell subsets included and lack of functional variation implicit in the immune response. Shen et al. investigated genomic data to develop an immune gene set-based prognosis signature in ovarian cancer [49], but they did not consider drug treatment. In pan-cancer analyses, important associations between the immune cell subset and survival [13,30] and response to checkpoint blockade

[50] across tumour types were uncovered using quantitative genomic techniques. In the present study, a deep knowledge was gained on the clinical significance of the immune response, especially on investigating the diverse association between survival after platinum chemotherapy with different functional immune cell subtypes and accounts for the effects of different molecular subtypes.

This retrospective study has some limitations. The primary limitation is that the relative populations of immune cell types were computationally estimated. To strengthen this, information should be measured directly. However, obtaining tumour-infiltrating immune cells in thousands of HGSOC samples with long-term follow-ups would be extremely research resource-intensive. In addition, some of the cohorts were profiled using platforms not formally confirmed for use with CIBERSORT. This condition may bring up some uncertainty on the estimated immune infiltrate proportions. The second limitation is the high missing rate for the clinical covariates, such as grade and stage, reducing the statistical power in multivariable Cox proportional hazard models. Meanwhile, various studies included in our study can increase the generalisability of our findings. This factor is also a limitation because the patients with HGSOC were from different regions and participated in different clinical settings. Considering that this condition is not ideal, only HGSOC samples who received platinum-based chemotherapy were included in our study. Finally, although the associations reported here arise from a pooled cohort, further biological experiments and validation in independent studies are required. Nevertheless, this study represents, to our knowledge, the largest study investigating immune cell infiltration and prognosis after platinum treatment in HGSOCs.

To conclude, this study has shown that a multitude of immune cells, such as M1 macrophages, M2 macrophages, CD8+ T cells are associated with the survival of patients with HGSOC treated with platinum-based chemotherapy in a large pooled cohort and using an unbiased in silico approach. These findings have the potential for identifying patients who can respond to immunotherapies, highlighting potential new drug targets and drug combination strategies.

## Acknowledgements

We thank the patients and investigators who participated in TCGA and GEO for providing data.

## Funding

This study was supported by two grants to RL: the National Scientific Foundation of China (no. 31801121) and Scientific Foundation of Xiang Ya hospital (2016Q04). RL contributed to the study design, performed statistical analysis, interpretation and drafted the manuscript.

## Declaration of Competing Interest

None.

## Ethics approval and consent to participate

This study has been approved by the Institute of Clinical Pharmacology, Xiangya Hospital, Central South University.

## Availability of data and materials

The datasets supporting the conclusions of this article are available in the public databases Gene Expression Omnibus (https://www.ncbi.nlm.nih.gov/gds/) with the accession numbers: GSE53963, GSE63885,GSE49997,GSE51088,GSE26712,GSE17260,GSE32062, GSE32063,GSE14764, GSE30161, GSE9891, GSE13876, TCGA/GSE821911. All these studies have been previously approved by their respective institutional review boards.

## Consent for publication

All authors have reviewed the manuscript and consented for publication.

## Supplementary materials

Supplementary material associated with this article can be found in the online version at doi:10.1016/j.ebiom.2019.102602.

## References

[1] Bray F, Ferlay J, Soerjomataram I, Siegel RL, Torre LA, Jemal A. Global cancer statistics 2018: Globocan estimates of incidence and mortality worldwide for 36 cancers in 185 countries. CA Cancer J Clin 2018;68(6):394–424.
[2] Ledermann JA, Raja FA, Fotopoulou C, Gonzalez-Martin A, Colombo N, Sessa C. Newly diagnosed and relapsed epithelial ovarian carcinoma: ESMO clinical practice guidelines for diagnosis, treatment and follow-up. Ann Oncol Off J Eur Soc Med Oncol 2013;24(Suppl 6):vi24–32.
[3] Seidman JD, Horkayne-Szakaly I, Haiba M, Boice CR, Kurman RJ, Ronnett BM. The histologic type and stage distribution of ovarian carcinomas of surface epithelial origin. Int J Gynecol Pathol Off J Int Soc Gynecol Pathol 2004;23(1):41–4.
[4] Miller DS, Blessing JA, Krasner CN, Mannel RS, Hanjani P, Pearl ML, et al. Phase II evaluation of pemetrexed in the treatment of recurrent or persistent platinum-resistant ovarian or primary peritoneal carcinoma: a study of the Gynecologic Oncology Group. J Clin Oncol 2009;27(16):2686–91.
[5] Allemani C, Matsuda T, Di Carlo V, Harewood R, Matz M, Niksic M, et al. Global surveillance of trends in cancer survival 2000-14 (CONCORD-3): analysis of individual records for 37 513 025 patients diagnosed with one of 18 cancers from 322 population-based registries in 71 countries. Lancet 2018;391(10125):1023–75.
[6] Integrated genomic analyses of ovarian carcinoma. Nature 2011;474(7353):609–15.
[7] Verhaak RG, Tamayo P, Yang JY, Hubbard D, Zhang H, Creighton CJ, et al. Prognostically relevant gene signatures of high-grade serous ovarian carcinoma. J Clin Invest 2013;123(1):517–25.
[8] Patch AM, Christie EL, Etemadmoghadam D, Garsed DW, George J, Fereday S, et al. Whole-genome characterization of chemoresistant ovarian cancer. Nature 2015;521(7553):489–94.
[9] Liu R, Zeng Y, Zhou CF, Wang Y, Li X, Liu ZQ, et al. Long noncoding RNA expression signature to predict platinum-based chemotherapeutic sensitivity of ovarian cancer patients. Sci Rep 2017;7(1):18.
[10] Heindl A, Sestak I, Naidoo K, Cuzick J, Dowsett M, Yuan Y. Relevance of spatial heterogeneity of immune infiltration for predicting risk of recurrence after endocrine therapy of ER+ breast cancer. J Natl Cancer Inst 2018;110(2).
[11] DeNardo DG, Ruffell B. Macrophages as regulators of tumour immunity and immunotherapy. Nat Rev Immunol 2019;19(6):369–82.
[12] Ali HR, Chlon L, Pharoah PD, Markowetz F, Caldas C. Patterns of immune infiltration in breast cancer and their clinical implications: a gene-expression-based retrospective study. PLoS Med 2016;13(12):e1002194.
[13] Iglesia MD, Parker JS, Hoadley KA, Serody JS, Perou CM, Vincent BG. Genomic analysis of immune cell infiltrates across 11 tumor types. J Natl Cancer Inst 2016;108(11).
[14] Fu Y, Liu S, Zeng S, Shen H. From bench to bed: the tumor immune microenvironment and current immunotherapeutic strategies for hepatocellular carcinoma. J Exper Clin Cancer Res 2019;38(1):396.
[15] Pu X, Wu L, Su D, Mao W, Fang B. Immunotherapy for non-small cell lung cancers: biomarkers for predicting responses and strategies to overcome resistance. BMC Cancer 2018;18(1):1082.
[16] Mahoney KM, Rennert PD, Freeman GJ. Combination cancer immunotherapy and new immunomodulatory targets. Nat Rev Drug Discov 2015;14(8):561–84.
[17] Wang W, Liu J, He Y, McLeod HL. Prospect for immune checkpoint blockade: dynamic and comprehensive monitorings pave the way. Pharmacogenomics 2017;18(13):1299–304.
[18] Brahmer JR, Tykodi SS, Chow LQ, Hwu WJ, Topalian SL, Hwu P, et al. Safety and activity of anti-PD-L1 antibody in patients with advanced cancer. N Engl J Med 2012;366(26):2455–65.
[19] Sato E, Olson SH, Ahn J, Bundy B, Nishikawa H, Qian F, et al. Intraepithelial CD8+ tumor-infiltrating lymphocytes and a high CD8+/regulatory T cell ratio are associated with favorable prognosis in ovarian cancer. Proc Natl Acad Sci USA 2005;102(51):18538–43.
[20] Zhang L, Conejo-Garcia JR, Katsaros D, Gimotty PA, Massobrio M, Regnani G, et al. Intratumoral T cells, recurrence, and survival in epithelial ovarian cancer. N Engl J Med 2003;348(3):203–13.
[21] Hwang WT, Adams SF, Tahirovic E, Hagemann IS, Coukos G. Prognostic significance of tumor-infiltrating T cells in ovarian cancer: a meta-analysis. Gynecol Oncol 2012;124(2):192–8.
[22] Newman AM, Liu CL, Green MR, Gentles AJ, Feng W, Xu Y, et al. Robust enumeration of cell subsets from tissue expression profiles. Nat Method 2015;12(5):453–7.
[23] Fan C, Oh DS, Wessels L, Weigelt B, Nuyten DS, Nobel AB, et al. Concordance among gene-expression-based predictors for breast cancer. N Engl J Med 2006;355(6):560–9.
[24] Rooney MS, Shukla SA, Wu CJ, Getz G, Hacohen N. Molecular and genetic properties of tumors associated with local immune cytolytic activity. Cell 2015;160(1–2):48–61.

[25] Sun GW, Shook TL, Kay GL. Inappropriate use of bivariable analysis to screen risk factors for use in multivariable analysis. J Clin Epidemiol 1996;49(8):907–16.
[26] Jerome Friedman TH, Tibshirani R. Regularization paths for generalized linear models via coordinate descent. J Stat Softw 2010;33(1):1–22.
[27] Team R.C.. R: a language and environment for statistical computing. Vienna, Austria: R Foundation for Statistical Computing; 2017.
[28] Coffelt SB, Wellenstein MD, de Visser KE. Neutrophils in cancer: neutral no more. Nat Rev Cancer 2016;16(7):431–46.
[29] Fridman WH, Zitvogel L, Sautes-Fridman C, Kroemer G. The immune contexture in cancer prognosis and treatment. Nat Rev Clin Oncol 2017;14(12):717–34.
[30] Gentles AJ, Newman AM, Liu CL, Bratman SV, Feng W, Kim D, et al. The prognostic landscape of genes and infiltrating immune cells across human cancers. Nat Med 2015;21(8):938–45.
[31] Darb-Esfahani S, Kunze CA, Kulbe H, Sehouli J, Wienert S, Lindner J, et al. Prognostic impact of programmed cell death-1 (PD-1) and PD-ligand 1 (PD-L1) expression in cancer cells and tumor-infiltrating lymphocytes in ovarian high grade serous carcinoma. Oncotarget 2016;7(2):1486–99.
[32] Webb JR, Milne K, Kroeger DR, Nelson BH. PD-L1 expression is associated with tumor-infiltrating T cells and favorable prognosis in high-grade serous ovarian cancer. Gynecol Oncol 2016;141(2):293–302.
[33] Aran D, Hu Z, Butte AJ. xCell: digitally portraying the tissue cellular heterogeneity landscape. Genome Biol 2017;18(1):220.
[34] Li B, Li T, Pignon JC, Wang B, Wang J, Shukla SA, et al. Landscape of tumor-infiltrating t cell repertoire of human cancers. Nat Genet 2016;48(7):725–32.
[35] Hao Y, Yan M, Heath BR, Lei YL, Xie Y. Fast and robust deconvolution of tumor infiltrating lymphocyte from expression profiles using least trimmed squares. PLoS Comput. Biol 2019;15(5):e1006976.
[36] Zhao SG, Lehrer J, Chang SL, Das R, Erho N, Liu Y, et al. The immune landscape of prostate cancer and nomination of PD-L2 as a potential therapeutic target. J Natl Cancer Inst 2019;111(3):301–10.
[37] Noy R, Pollard JW. Tumor-associated macrophages: from mechanisms to therapy. Immunity 2014;41(1):49–61.
[38] Zhang M, He Y, Sun X, Li Q, Wang W, Zhao A, et al. A high M1/M2 ratio of tumor-associated macrophages is associated with extended survival in ovarian cancer patients. J Ovarian Res 2014;7:19.
[39] Zhu Y, Knolhoff BL, Meyer MA, Nywening TM, West BL, Luo J, et al. CSF1/CSF1R blockade reprograms tumor-infiltrating macrophages and improves response to T-cell checkpoint immunotherapy in pancreatic cancer models. Cancer Res. 2014;74(18):5057–69.
[40] Pang Y, Gara SK, Achyut BR, Li Z, Yan HH, Day CP, et al. TGF-beta signaling in myeloid cells is required for tumor metastasis. Cancer Discov 2013;3(8):936–51.
[41] Jablonska J, Leschner S, Westphal K, Lienenklaus S, Weiss S. Neutrophils responsive to endogenous IFN-beta regulate tumor angiogenesis and growth in a mouse tumor model. J Clin.Invest 2010;120(4):1151–64.
[42] Kaech SM, Cui W. Transcriptional control of effector and memory CD8+ T cell differentiation. Nat Rev Immunol 2012;12(11):749–61.
[43] Kurachi M. CD8+ T cell exhaustion. Semin Immunopathol 2019;41(3):327–37.
[44] Kamphorst AO, Wieland A, Nasti T, Yang S, Zhang R, Barber DL, et al. Rescue of exhausted CD8 T cells by PD-1-targeted therapies is CD28-dependent. Science (New York, NY) 2017;355(6332):1423–7.
[45] Goode EL, Block MS, Kalli KR, Vierkant RA, Chen W, Fogarty ZC, et al. Dose-Response association of CD8+ tumor-infiltrating lymphocytes and survival time in high-grade serous ovarian cancer. JAMA Oncol 2017;3(12):e173290.
[46] Silva-Santos B, Serre K, Norell H. $\gamma\delta$ T cells in cancer. Nat Rev Immunol 2015;15:683.
[47] Truxova I, Kasikova L, Hensler M, Skapa P, Laco J, Pecen L, et al. Mature dendritic cells correlate with favorable immune infiltrate and improved prognosis in ovarian carcinoma patients. J Immunother Cancer 2018;6(1):139.
[48] Drakes ML, Stiff PJ. Regulation of ovarian cancer prognosis by immune cells in the tumor microenvironment. Cancers 2018;10(9).
[49] Shen S, Wang G, Zhang R, Zhao Y, Yu H, Wei Y, et al. Development and validation of an immune gene-set based prognostic signature in ovarian cancer. EBioMedicine 2019;40:318–26.
[50] Charoentong P, Finotello F, Angelova M, Mayer C, Efremova M, Rieder D, et al. Pan-cancer immunogenomic analyses reveal genotype-immunophenotype relationships and predictors of response to checkpoint blockade. Cell Rep 2017;18(1):248–62.